Electronic supplementary information for

Relationship between crosslinking and ordering for the fabrication of soft templated (FDU-16) mesoporous carbon thin films

Yuanzhong Zhang, Zhe Qiang, and Bryan D. Vogt

Department of Polymer Engineering, University of Akron, Akron, OH 44325

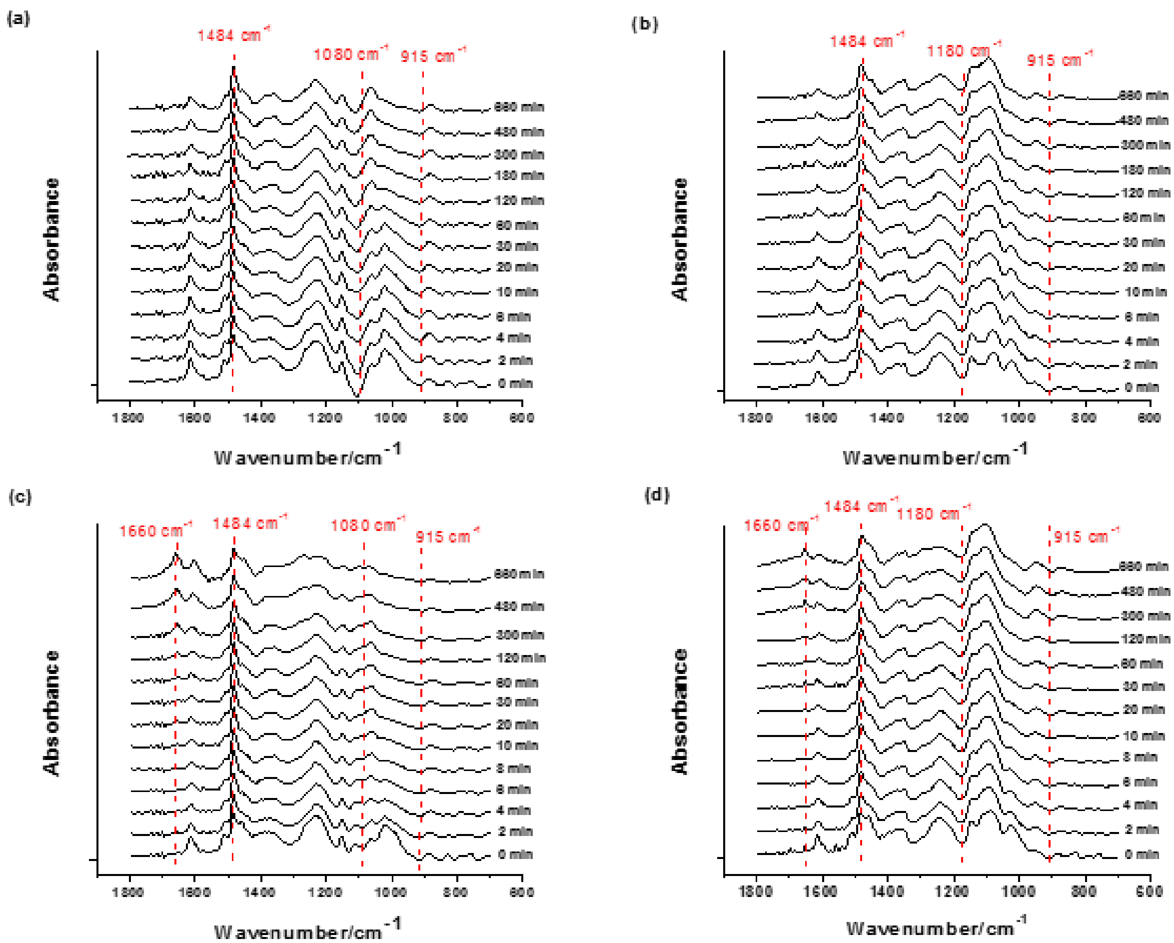

Figure S1. Temporal evolution of the FTIR spectra for (a) resol, (b) FDU-16 films at 100 °C and when crosslinking at 140 °C for (c) resol and (d) FDU-16 films.

Table S1. FTIR bands assignment (Full)	
Wavenumber of observed peak centers or bands (cm^{-1})	**Functional group**
1740-1590 (doublet)	C=O substitution on aromatic ring[30]
1625-1590	aromatic C=C stretching vibration due to asymmetric substitution[30]
1511	aromatic C=C stretching in 1,4 or 1,2,4 substituted benzene ring[30]
1484	aromatic C=C stretching[28]
1460	CH_2 deformation vibration in -CH_2-OH[30]
1410-1310	COH bending vibration of phenol[30]
1374	-CH2- symmetric deformation in F127[31]
1360	-CH2- wag, C-C stretching in F127[31]
1343	-CH2- wag in F127[31]
1260-1180	CO stretching of phenol[30]
1175-1150	CO stretching of o- and p- alkyl phenols[30]
1149	C-O-C stretching and C-C stretching in F127[31]
1113	C-O-C stretching in F127[31]
1070-1050	C-O-C stretching in both phenolic resin and F127[31]
1028; 1011; 995	δ(O-H)ν(C-O) vibration of 2, 4, 6-trihydroxymethylphenol[29]
1020; 996; 990	δ(O-H)ν(C-O) vibration of 2, 4-dihydroxymethylphenol[29]
1010	δ(O-H)ν(C-O) vibration of 2, 6-dihydroxymethylphenol[29]
1003; 995	δ(O-H)ν(C-O) vibration in primary alcohol of 2-hydroxymethylphenol[29]
991	δ(O-H)ν(C-O) vibration of 4-hydroxymethylphenol[29]
963	CH2 rock[31]
947	CH2 rock and C-O-C stretching[31]
890	aromatic =C-H out-of-plane deformation vibration, 2, 4, 6- substituted phenol[30]
830	4- or 2, 4- substituted phenol[30]
756	2- substituted phenol[30]

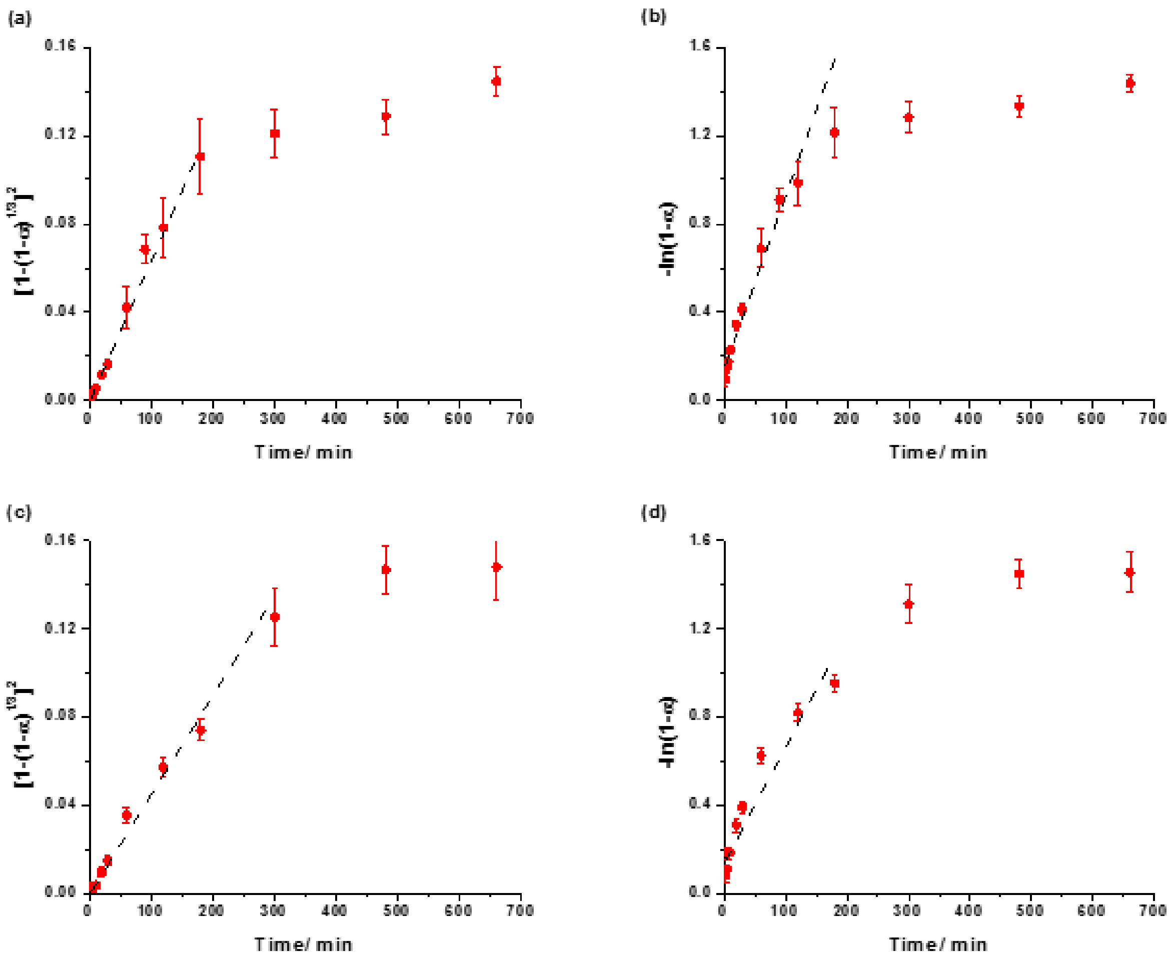

Figure S2. Integral fitting of resol (a,b) and FDU-16 (c, d) at 100 °C to (a,c) the Jander model and (b, d) 1st order reaction model.

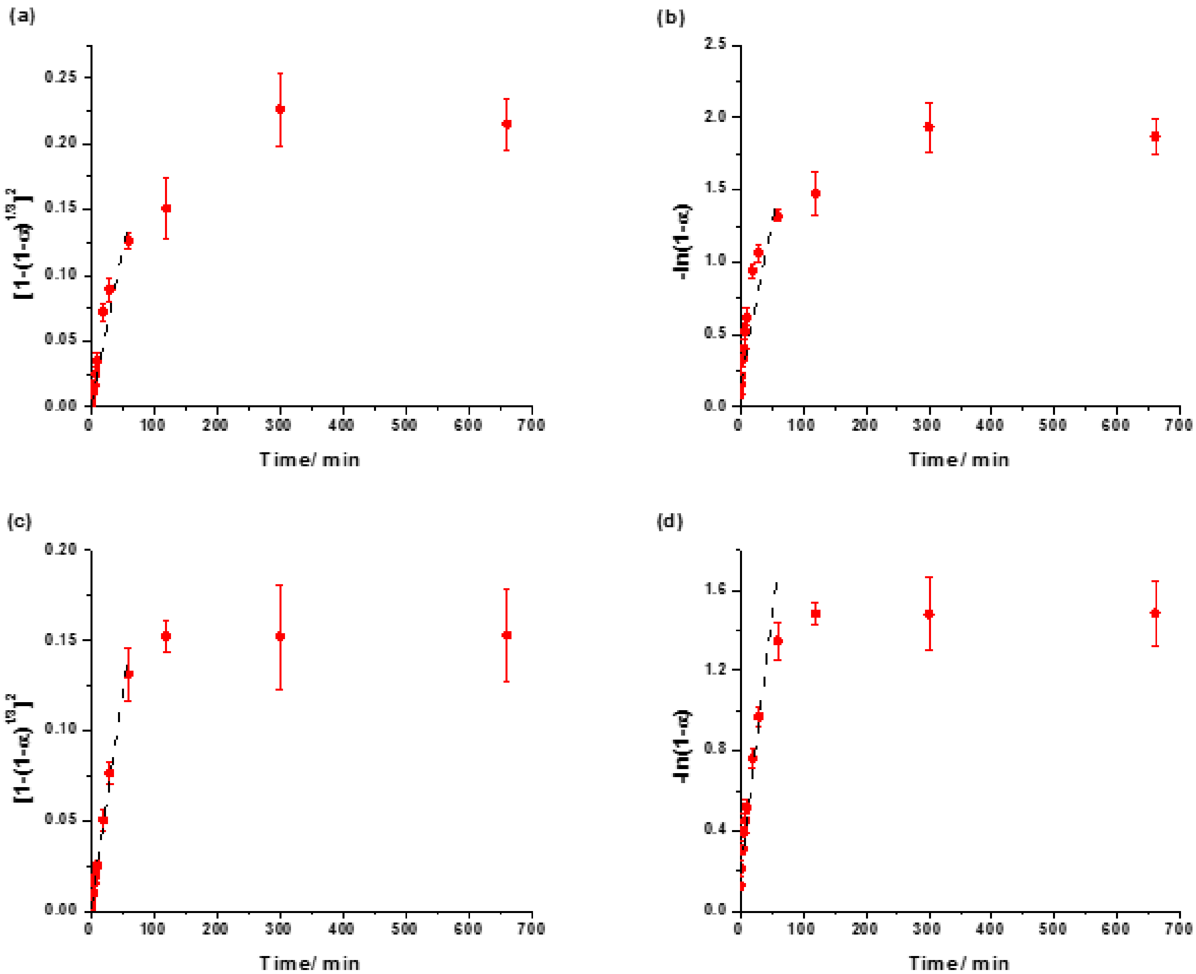

Figure S3. Integral fitting of resol (a,b) and FDU-16 (c, d) at 120 °C to (a,c) the Jander model and (b, d) 1st order reaction model

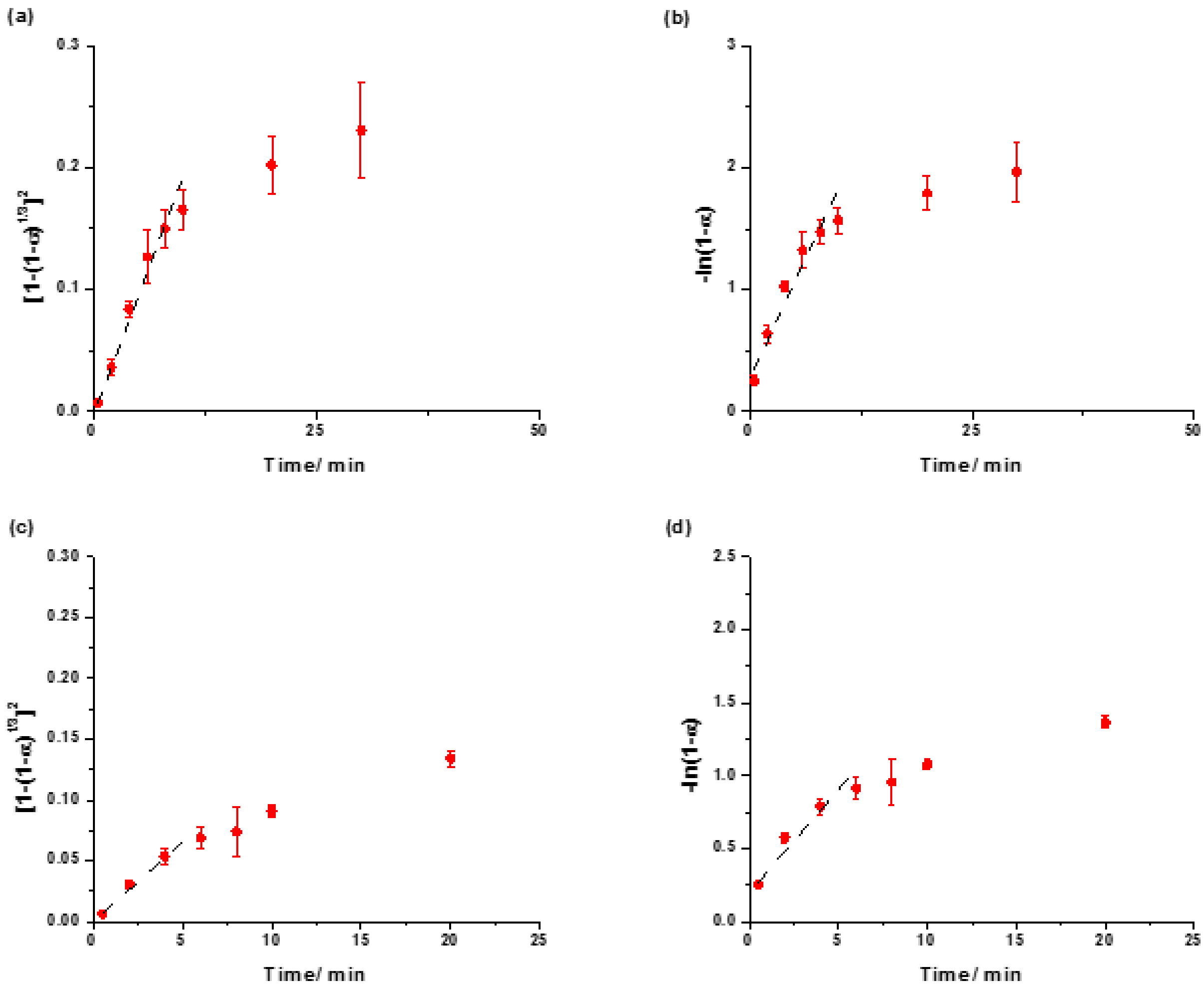

Figure S4. Integral fitting of resol (a,b) and FDU-16 (c, d) at 140 °C to (a,c) the Jander model and (b, d) 1st order reaction model

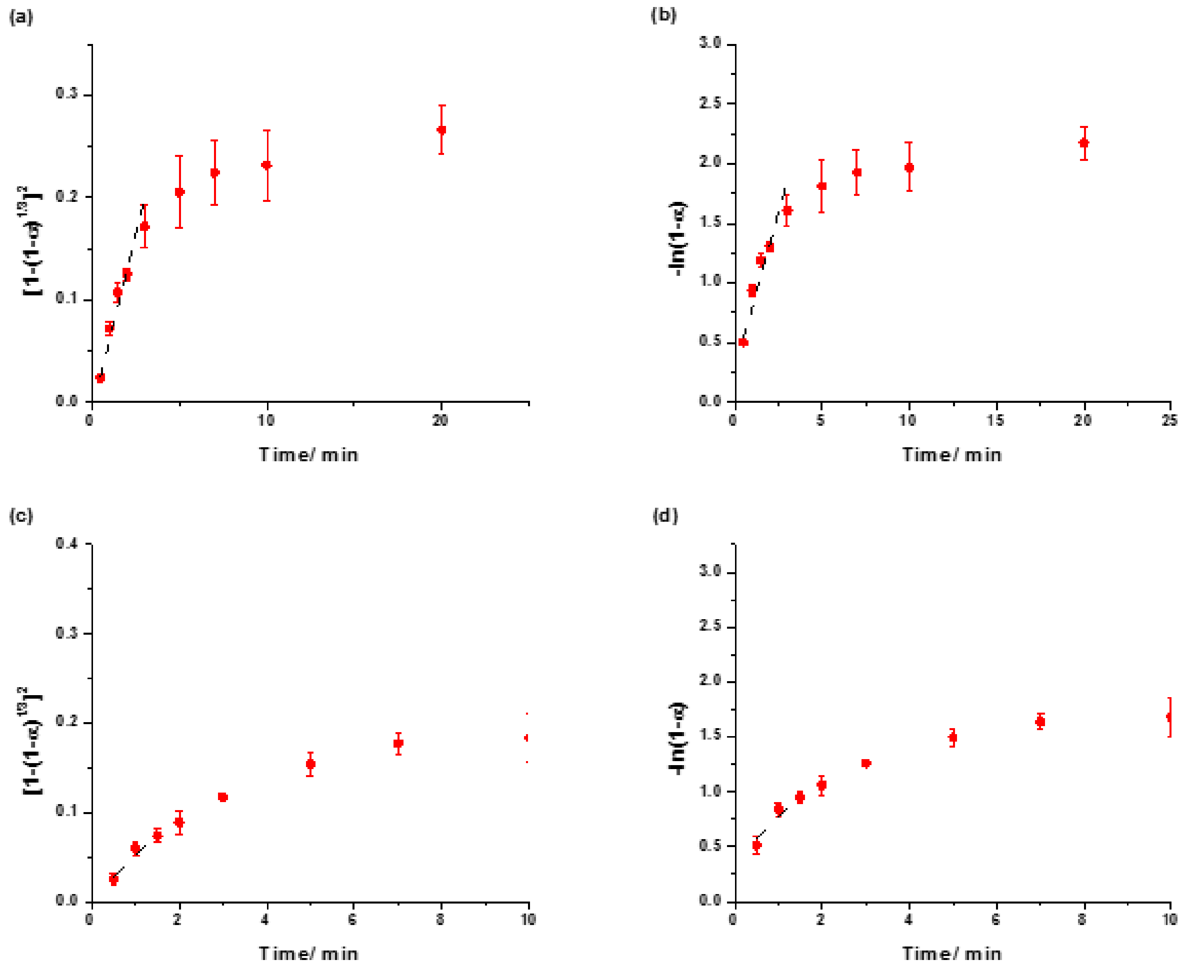

Figure S5. Integral fitting of resol (a,b) and FDU-16 (c, d) at 160 °C to (a,c) the Jander model and (b, d) 1st order reaction model

Table S2. Details of integral fitting result

	INTERCEPT	SLOPE (rate constant)	ADJ. R^2	FITTING RANGE (MAXIMUM)
100 ^{o}C				
RESOL (JANDER)	$-6.21X10^{-4}$	$6.38X10^{-4}$	0.977	2-180 min
RESOL (1^{ST} ORDER)	0.143	0.00782	0.973	2-180 min
FDU-16 (JANDER)	$-4.20X10^{-4}$	$4.51X10^{-4}$	0.977	2-300 min
FDU-16 (1^{ST} ORDER)	0.143	0.0049	0.905	2-300 min
120 ^{o}C				
RESOL (JANDER)	$-2.31X10^{-4}$	0.00237	0.950	0.5-60 min
RESOL (1^{ST} ORDER)	0.153	0.0221	0.868	0.5-60 min
FDU-16 (JANDER)	$4.64X10^{-4}$	0.0024	0.995	0.5-60 min
FDU-16 (1^{ST} ORDER)	0.179	0.0254	0.913	0.5-60 min
140 ^{o}C				
RESOL (JANDER)	-0.00238	0.0194	0.981	0.5-10 min
RESOL (1^{ST} ORDER)	0.269	0.156	0.914	0.5-10 min
FDU-16 (JANDER)	$3.38X10^{-4}$	0.01311	0.971	0.5-6 min
FDU-16 (1^{ST} ORDER)	0.198	0.142	0.911	0.5-6 min
160 ^{o}C				
RESOL (JANDER)	-0.00911	0.06867	0.972	0.5-3 min
RESOL (1^{ST} ORDER)	0.279	0.524	0.940	0.5-3 min
FDU-16 (JANDER)	0.00295	0.0498	0.971	0.5-1.5 min
FDU-16 (1^{ST} ORDER)	0.363	0.413	0.800	0.5-1.5 min

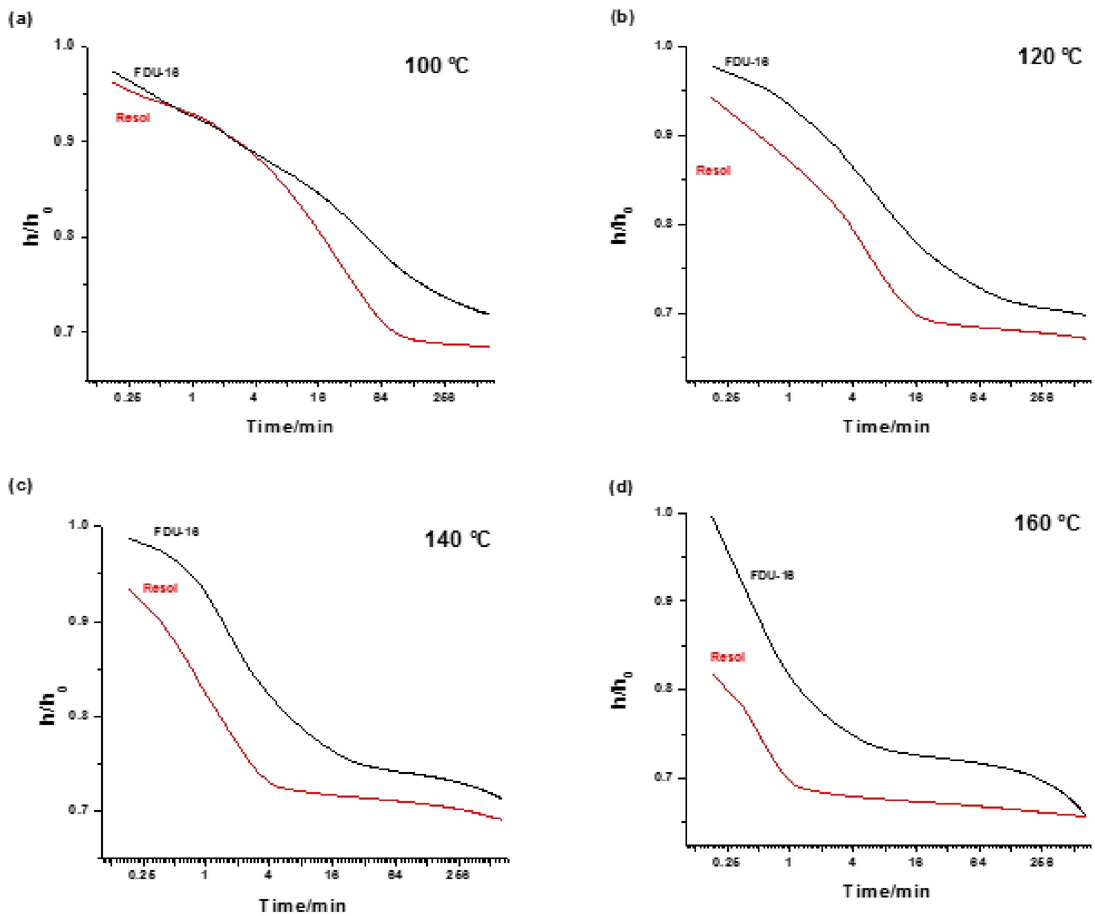

Figure S6. In-situ ellipsometry data of normalized film thickness at (a) 100 °C (b) 120 °C (c) 140 °C (d) 160 °C.

(a)

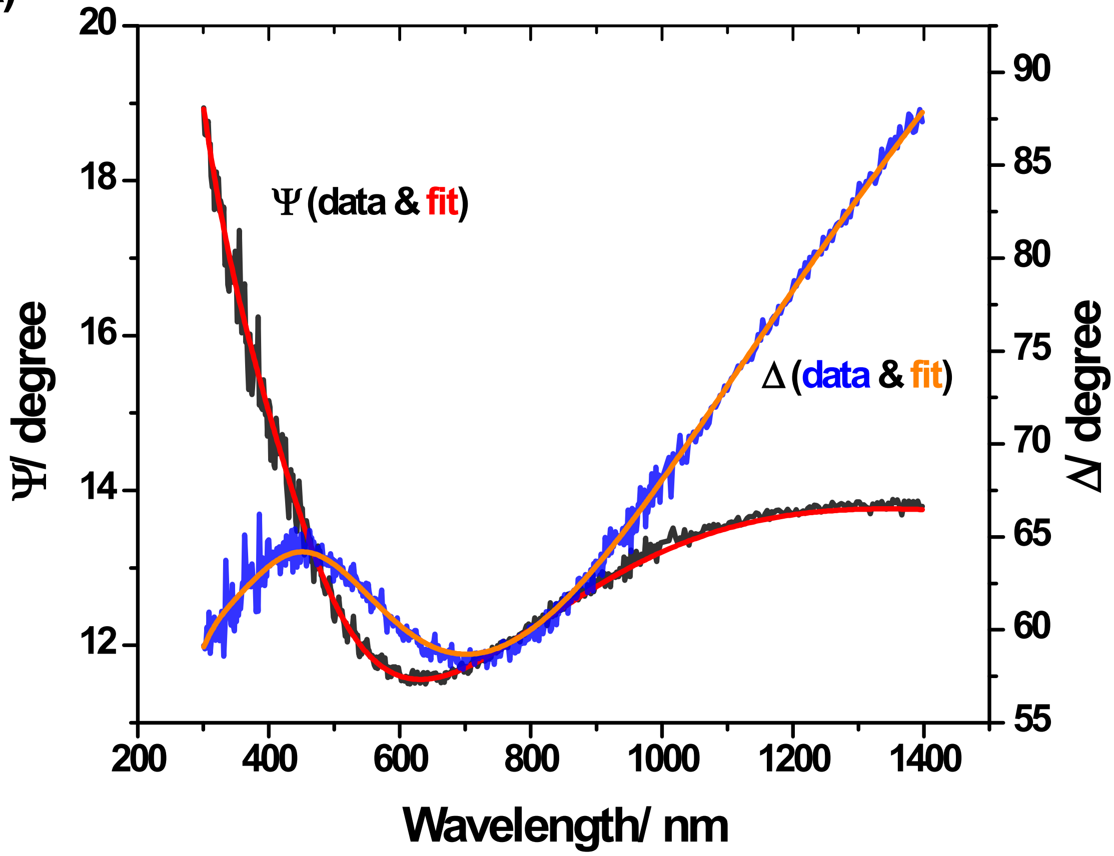

Ψ (data & fit)
Δ (data & fit)
Ψ/ degree
Δ/ degree
Wavelength/ nm
20
18
16
14
12
90
85
80
75
70
65
60
55
200
400
600
800
1000
1200
1400

(b)

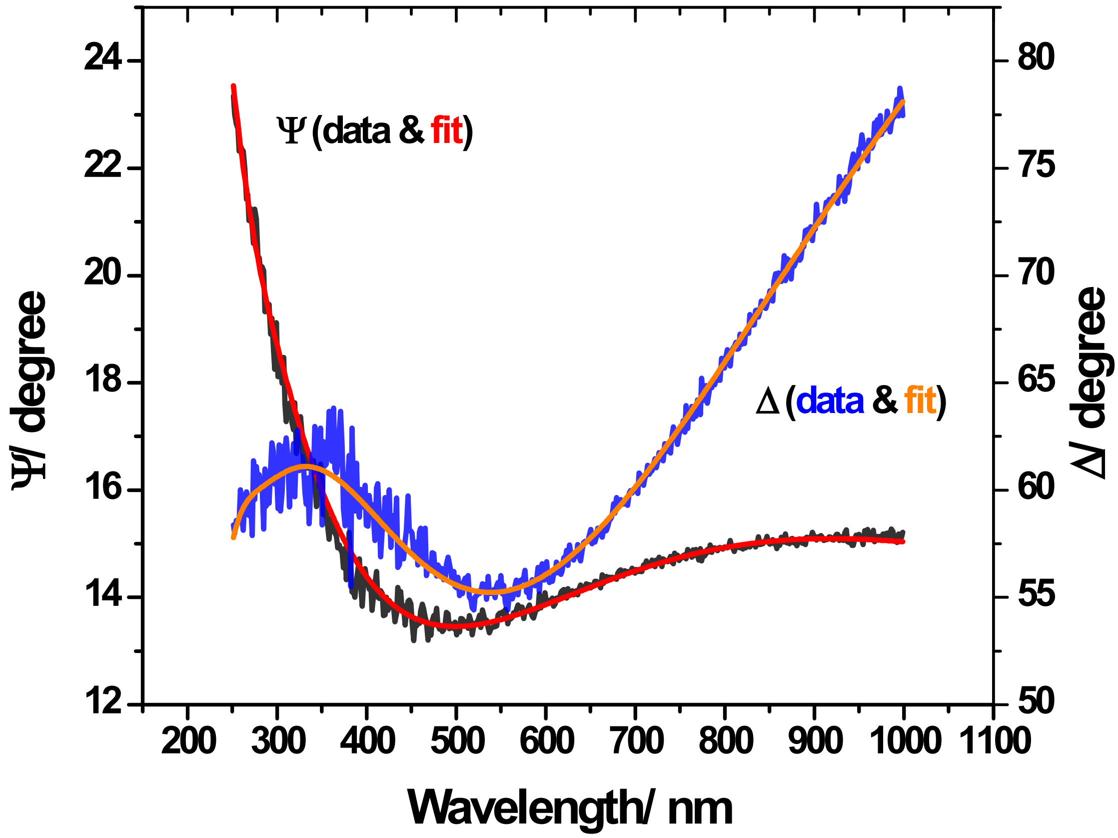

Figure S7. Ellipsometric angles (Ψ, Δ) and fitting at incident angle of 70 º for mesoporous carbon based on FDU-16 using (a) standard heating protocol of 120 °C for 24 h and (b) accelerated heating of 100 °C for 1.5 h and then 160 °C for 1.5 h. Both films are carbonized at 800 °C. The dashed lines indicate the recursive fit to the data.

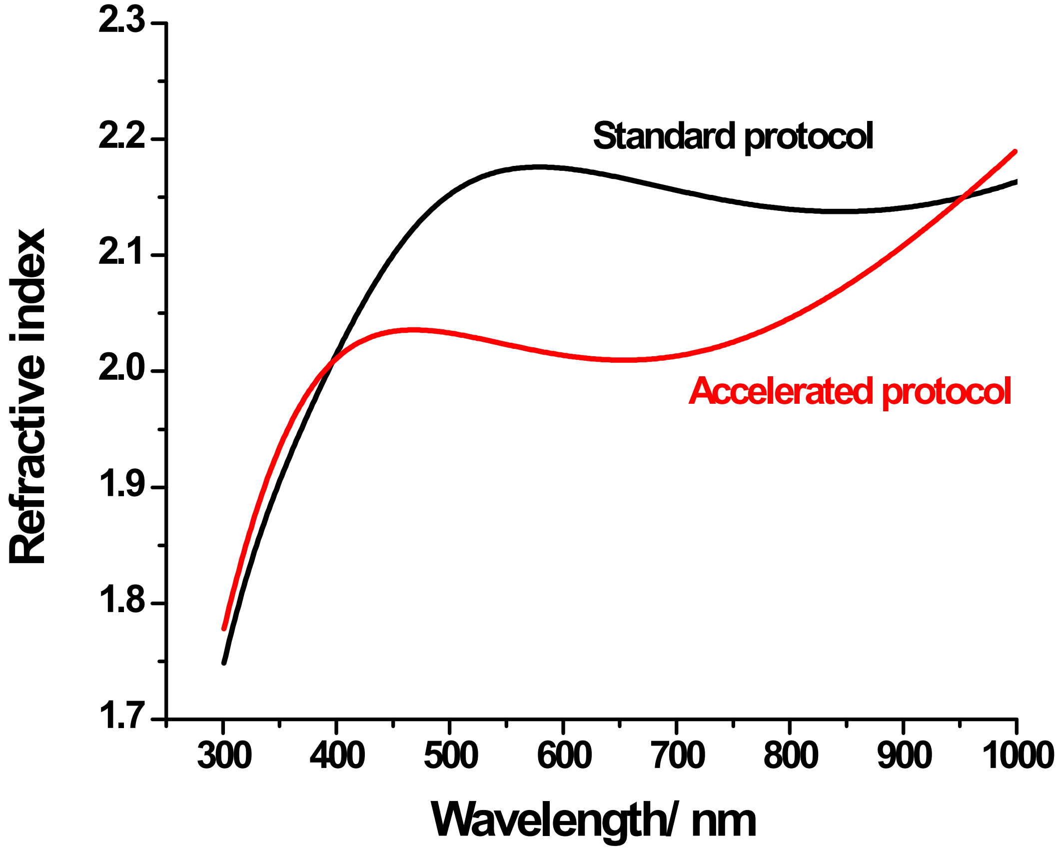

Figure S8. Refractive index of mesoporous carbon films as determined from ellipsometry shown in Figure S7.